

Ship-borne ceilometer measurements over the northwestern Pacific and the Indian sector of the Southern Ocean, and at Syowa Station, Antarctica, in the summers of 2010/11 to 2019/20

Naohiko HIRASAWA^{1,2*}, Masataka SHIOBARA^{1,2**}, Toshiyuki MURAYAMA³, and Hiroshi KOBAYASHI⁴

¹ National Institute of Polar Research, Research Organization of Information and Systems, 10-3 Midori-cho, Tachikawa, Tokyo 190-8518.

² Department of Polar Science, School of Multidisciplinary Sciences, SOKENDAI (The Graduate University for Advanced Studies), 10-3 Midori-cho, Tachikawa, Tokyo 190-8518.

³ Faculty of Marine Technology, Tokyo University of Marine Science and Technology, 2-1-6 Etchujima Koto-ku, Tokyo 135-8533.

⁴ Graduate Faculty of Interdisciplinary Research, University of Yamanashi, 4-4-37 Takeda, Kofu, Yamanashi 400-8510.

*Corresponding author. Naohiko Hirasawa (hira.n@nipr.ac.jp)

**Currently retired

(Received April 26, 2022; Accepted September 13, 2022)

Abstract: The present study examined ship-borne ceilometer data collected over the northwestern Pacific Ocean, Indian Southern Ocean, and Syowa Station (69°00' S, 39°35' E), Antarctica. The ceilometer observation provides information on clouds and precipitation, especially under clouds on the oceans, where very little information is, and the data are significant for identifying the present state of the warming climate and estimating the future change of the climate. The observations were conducted over the course of ten annual cruises aboard the icebreaker *Shirase* as part of the Japanese Antarctic Research Expedition (JARE) program from November to April. The first cruise departed Tokyo, Japan, in November 2010. Observations were then conducted annually until November 2019. Ceilometers emit light vertically upward and measure the intensity of backscattered light in the atmosphere. The obtained data include the vertical profiles of the backscatter intensity, estimated cloud-base heights for each profile, and parameters such as time, location, etc. Here, we publish four different datasets comprising the obtained data as follows: daily files in the manufacturer's format, annual cruise files in the manufacturer's format, daily files with decimal expression processed in the projects, and annual cruise files with hourly averaged and decimal expression processed in the

projects. The data can be obtained from the National Institute of Polar Research (NIPR) at <https://doi.org/10.17592/002.2022100393>

1. Background & Summary

The Japanese Antarctic Research Expedition (JARE) program conducts annual cruises between Japan and Antarctica from November to April. Ship-borne ceilometer observations were carried out from the 52nd JARE cruise (JARE-52, November 2010 to April 2011) to the 61st JARE cruise (JARE-61, November 2019 to April 2020) aboard the Japanese polar research vessel, the “*Shirase*”. During the period, the ceilometer observation was continued in conjunction with several scientific projects as follows: “Aerosol-mediated material cycle processes in the Antarctic coastal region and the Southern Ocean” (Project No.: AP-11) on JARE-52 (December 2010–March 2011) to JARE-57 (December 2015–March 2016), “Changing of East Antarctic aerosols in the global biogeochemical environment” (Project Nos.: AP0910 and AP0932) and “Mechanism of variation in the surface condition of the ice sheet and heat and moisture budget in east Antarctica” (Project No.: AP0911) on JARE-58 (December 2016–March 2017) to JARE-61 (December 2019–March 2020). The cruise tracks pass through the northwestern Pacific Ocean, through the Indian Southern Ocean, to Syowa Station, Antarctica (Fig. 1a).

The progression of global warming is associated with a variety of climatic feedbacks, the effects of which need to be clarified in order to predict future changes in climate. Although several Intergovernmental Panel on Climate Change (IPCC) reports^{1,2} have shown that aerosol-cloud-radiation processes are the most complex of these climate feedbacks, it is not yet known whether these aerosol-cloud-radiation processes will have a positive or negative effect on global warming. Cloud properties, such as distribution, thickness, particle size, and the ice/liquid ratio of cloud particles all affect both short-wave and long-wave radiation processes, and the cloud properties themselves vary depending on the nature of the aerosols that act as cloud nuclei.

One of the most important issues about Antarctica related to global warming is the mass balance of the Antarctic ice sheet (AIS), which is a major player in sea level change. To understand the present state of mass balance between the sea and the AIS, we need to obtain more precipitation data and know its regional distribution. Recently, observations using radars^{3,4,5} and ceilometers⁶ have been carried out, and it is very important to continue such efforts.

While satellite observations are indispensable for examining the present state of clouds and precipitation around the globe, ground-based observations are required in order to verify the satellite data^{7,8}. However, few such observations have been performed in the Antarctic region and over the oceans. Given this context, the “*Shirase*”, which travels between Antarctica and Japan every year, is well suited for use as a platform for surface-based observations over the ocean. We have therefore installed a ceilometer on the *Shirase* to continuously observe the vertical profiles of clouds and their

properties and precipitation. The obtained datasets represent a kind of cloud and precipitation climatology (e.g., cloud fractions along the cruise route^{9,10}) for the Antarctic region and will be valuable for validating climate models.

2. Location and period of the observation

[Figure 1](#) shows the cruise tracks that are typically used by the *Shirase*; the vessel departs from Japan for Fremantle (Australia), Syowa Station (Antarctica), and Sydney (Australia) before returning to Japan. The ceilometer data along the red transect has been archived, but no data was collected along the dashed black line as these areas are within the Exclusive Economic Zone (EEZ) of each country.

[Table 1](#) summarizes the locations and observation periods over which the measurements described in this study were conducted. The data is formatted in chronological order as follows: data from the northwestern Pacific leaving Japan (North Pacific in [Table 1](#)) was collected in November, data from Fremantle to Syowa Station over the Southern Ocean higher latitudes than approximately 41°S was collected in December (Fremantle to Syowa Station), data from Syowa Station (69°00' S, 39°35' E) was collected in January, data from Syowa Station to Sydney over the Southern Ocean at latitudes higher than approximately 45°S was collected in February and March (Syowa Station to Sydney), and data from the northwestern Pacific heading to Japan was collected in April (North Pacific). Blanks in the data reflect periods when the *Shirase* was within the EEZ of another country. On JARE-57, since the *Shirase* went to Cape Town after departing from Syowa Station and then went to Sydney through the Antarctic area, the cruise route with the data is divided into three portions (*1, *2, and *3 in [Table 1](#)) by the EEZs of South Africa.

3. Methods

Data were obtained by a ceilometer, which is a lidar system that is typically used to detect cloud base height at airports. The ceilometer (CL51, Vaisala Co. Ltd., Finland) used in this study was installed on the roof deck of the *Shirase* ([Fig.1b](#)). The technical and theoretical terms used in this manuscript follow those in the ceilometer instrument manual¹¹.

[Table 2](#) summarizes the main specifications of the observations. The ceilometer emits laser pulses in a vertical direction and measures the intensity of the backscatter caused mainly by precipitation and clouds. The emission frequency (inverse of the time interval of the laser emission) is 6.5 kHz, and the ceilometer records the measurement data most frequently every 6 seconds through the analysis of all the detected data. In this data archive, different record intervals have been chosen for each cruise, and the range (30s to 120s) is listed in [Table 2](#).

If the densities of cloud particles are so high that the laser beam cannot penetrate the cloud layer, then it is not possible to obtain meaningful signals beyond the bottom of the cloud layer.

According to the instrument manual¹¹, the instantaneous intensity of the return signal of the lidar can be estimated using the following equation:

$$Pr(z) = E_o \cdot \frac{c}{2} \cdot \frac{A}{z^2} \cdot \beta(z) \cdot e^{-2 \int_0^z \sigma(z') dz'} \quad (\text{eq. 1}),$$

where, z is the distance of a targeted air parcel (m), $Pr(z)$ is the instantaneous intensity received from distance z , E_o is the effective pulse energy (taking all optics attenuation into account; unit: Ws), c is the speed of light (unit: m s⁻¹), A is the receiver aperture (m²), $\beta(z)$ is the volume backscatter coefficient at distance z (unit: m⁻¹·sr⁻¹), and $\sigma(z')$ is the extinction coefficient (i.e., the attenuation factor in the forward direction) of distance z' (unit: m⁻¹). When $\sigma(z')$ is zero for every air parcel, which is indicative of a clear atmosphere, the two-way atmospheric transmittance is 1 ($e^0=1$), which means that there no attenuation of the light path in the air. The ceilometer records the vertical profile of the instantaneous intensity, $Pr(z)$, up to a height of 15,400 m and an interval of 10 m.

To estimate the backscatter coefficient, $\beta(z)$, using $Pr(z)$, the ceilometer assumes a linear relationship between the backscatter and extinction coefficient, and that the ratio, k , is constant over the observation range, as shown in eq. 2.

$$\beta(z) = k \cdot \sigma(z) \quad (\text{eq. 2}),$$

Using eq. 2, it is now possible to obtain the vertical profiles of the backscatter coefficient and the extinction coefficient from eq. 1.

The ceilometer detects the cloud bases using the vertical changes of the extinction coefficients. The change threshold values have been derived empirically by the manufacturer. In the present study, the three lowest cloud base heights are recorded.

4. Data Records

The data were recorded approximately every 30–90 seconds, including up to three cloud base heights and vertical profiles of backscattering coefficients. In addition to these observation data, the date, time and status information such as the tilt angle of the instrument are also recorded.

[Figure 2](#) shows examples of a month-long (February 2020, [Fig.2a](#)) and a day-long (February 22, 2020, [Fig.2b](#)) time-height sections. During most of the period in [Fig.2a](#), vertical distributions of clouds and precipitation are captured up to the highest altitude of the observation range. This is due to the fact that the optical thickness of Antarctic clouds is generally not large. The backscatter coefficients are shown in five different colors according to their magnitude. Periods that the colored area touches the ground indicate precipitation (e.g., February 22, 01-05 and 19-22 UTC in [Fig.2b](#)).

This section describes how these data are recorded in files and the directory structure of the data archive. The FTP site is <http://polaris.nipr.ac.jp/~aerosol01/open/ceilometer/>. The “ceilometer”

directory is the top directory of this dataset. Under the “ceilometer” directory, there are ten sub-directories for each JARE, for example, “JARE-52”, “JARE-53”, etc. In each of these sub-directories, we prepared four formats of time series data for each JARE cruise, and these are described in detail below.

(1) Daily files in Vaisala format

These are the original files outputted by the ceilometer. As the data contents and format are described in detail in the instrument manual¹¹, we provide only a brief description here in association with [Fig. 3a](#). The figure was constructed using representative portions of the file for 31 January 2017. The directory name is “0_daily” and file naming follows the following format, “S61101.DAT” for 1 November 2016 and “S70131.DAT” for 31 January 2017. In “S6” and “S7”, “S” has no meaning here and “6” and “7” represent the first digit of the year.

The file “S70131.DAT” starts with the following two lines:

```
-Ceilometer Logfile
-File created: 2016/11/01 3:37:34
```

The words in “Line 1” in [Fig. 3a](#), which is the first line of the file, are fixed. “Line 2” gives the date and the time (in Universal Time, [UT] format) of when the file was created.

The data set of the first observation is recorded in the following six lines, i.e., “Line 3” to “Line 8”. Subsequent data sets are recorded using 6 lines in the same way, with a blank line in between. “Line 11” is the last line of the file.

The quality of all measurement data depends on the performance of the instrument. The instrument outputs not only observed data but also a variety of information related to data quality. A representative sample of this information is given in “Line 5” and “Line 6” in [Fig. 3a](#) below. First, we will pick up and explain the observation data and such important information among the data recorded in lines 5 and 6. Other information that does not directly affect observations is not described here (see the instrument manual¹¹).

```
Line 5: 2W 00030 01850 ///// 00000400C080
```

The first character in “Line 5” (2) indicates the cloud base detection status as follows:

- 0: No significant backscatter
- 1: One cloud base detected
- 2: Two cloud bases detected
- 3: Three cloud bases detected
- 4: Full obscuration detected, but no cloud base detected
- 5: Some obscuration detected, but determined to be transparent

/: Raw data input to algorithm missing or suspect

The second character in “Line 5” (W) indicates the instrument status as follows:

0: Self-check OK

W: At least one warning active, no alarms

A: At least one alarm active

00030: The first cloud base height was 30 m.

01850: The second cloud base height was 1850 m.

/////: A third cloud base was not detected.

Line 6: 00100 10 1540 101 +26 080 01 0006 L0032HN15 159

00100: Resolution scale of the signal. The unit of the recorded backscatter coefficients for the resolution scale of “00100”, which is the standard value, is $(10^5 \cdot \text{sr} \cdot \text{km})^{-1}$.

10: Backscatter profile resolution in meters.

1540: Number of samples in the profile.

101: Laser pulse energy ratio (%) for the nominal factory setting.

+26: Laser temperature ($^{\circ}\text{C}$).

080: Window transmission estimate (%).

01: Tilt angle of the laser from vertical (degrees).

Line 7: 04f7b0776607fe802507007f3001190004e0003a0002a00024 ($5 \times 1540 + 2$ bytes)

04f7b: The backscatter intensity of the lowermost layer with a thickness of 10 m. The backscatter is two-way attenuated with a normalized sensitivity unit (basically, $100000 \cdot \text{sr} \cdot \text{km})^{-1}$ and coded with a 20-bit HEX ASCII character set.

07766: Same as above, but for the second lowest layer.

A total of 1540 sets of five characters are repeated up to the highest layer.

(2) Annual cruise files in Vaisala format

From the above daily files, we created a single data file for each cruise, consisting of hourly sample data. The data format is the same as the daily files. The directory name is “0_all” and the file naming follows the following format, “JARE58_hour.DAT” for the JARE-58 cruise from 1 November 2016 to 22 March 2017 (see [Table 1](#)).

(3) Daily files with decimal expression

The data in the daily files were derived from the Vaisala’s daily files. The directory name is “10_daily” and file naming follows the following format, “20170131.DAT” for 31 January 2017.

[Figure 3b](#) shows the data format for 31 January 2017. The 4 lines in the figure are recorded in 1 line in the actual files. The file is saved in CSV format with fixed record lengths. Compared with [Fig.](#)

[3a](#), the first column (2017) to the sixth column (05) are the date and time copied from the “Line 3”. The seventh column (69.03690) is the southern latitude (°S) and the eighth column (38.85789) is the eastern longitude (°E) of the position where the observation was made. From the ninth column (2W) to the 23rd column (159) are copies of the data contained in lines “Line 5” and “Line 6”. The 24th column (20347) is the decimal representation of the first column (04f7b) in “Line 7” in [Fig. 3a](#). Each column has a width of seven characters.

(4) Annual cruise files with hourly mean and decimal expression

We created a single data file for each cruise, consisting of hourly averaged data from the daily files in (3) above. The data format is the same as the daily files. The directory name is “10_all” and file naming follows the following format, for example, “JARE58_latlon.DAT” for the JARE-58 cruise from 1 November 2016 to 22 March 2017 (see [Table 1](#)).

[Figure 3c](#) shows the line format for data collected on 31 January 2017, 00:00. The 4 lines in the figure are recorded in 1 line in the actual files. The first column (2017) to the 22nd column (160) are copies of the same columns in the processed daily file at the corresponding time. The 23rd column (9033) is the average for 30 January 2017, 23:30 to 31 January 2017, 00:30.

5. Technical validation

(1) Caution regarding the use of the vertical profile data

In the event that a cloud is too thick for the laser beam from the ceilometer to penetrate, no observations beyond the cloud will be possible. Consequently, in vertical profile data, the data above the cloud base is meaningless. Similarly, the laser beam of the ceilometer may be unable to penetrate the heavy blowing snow that is commonly observed in polar regions. Therefore, care should be taken if there are such layers of high backscatter coefficients in the vertical profile.

(2) Unit of the recorded backscatter coefficients

The first word in the “line 6” in [Fig. 3a](#) indicates a resolution scale of the signal as explained in the previous section. The word is “01000” only in JARE-52, the first cruise of this project. And, that in other cruises is “00100”, which is the standard value of the instrument. Therefore, the unit of the recorded backscatter coefficients for JARE-52 is $(10^6 \cdot \text{sr} \cdot \text{km})^{-1}$ but $(10^5 \cdot \text{sr} \cdot \text{km})^{-1}$ for all other JARE cruises.

6. Figures

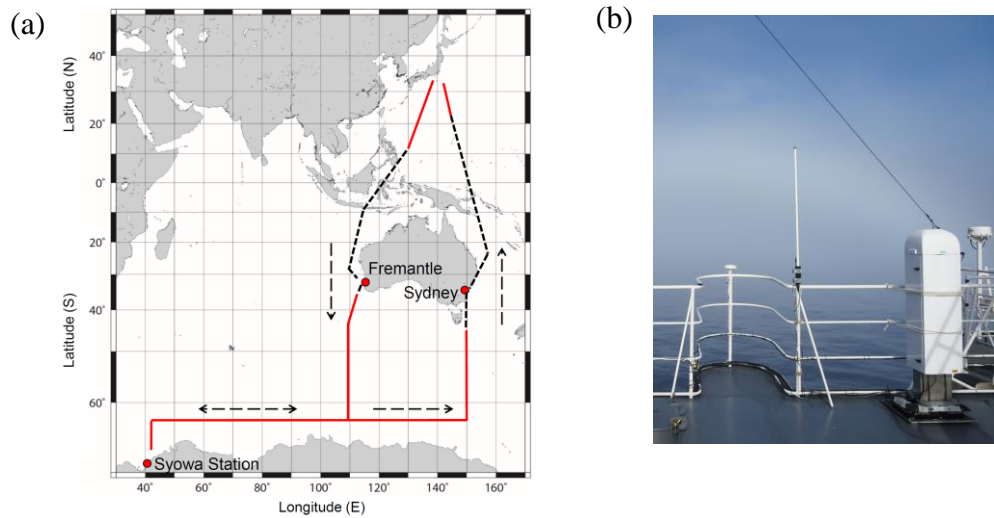


Figure 1. (a) Schematic representation of the most commonly used cruise tracks of the Japanese icebreaker *Shirase* from Japan to Fremantle (Australia), Syowa Station (Antarctica), and Sydney (Australia) before returning to Japan. The ceilometer data along the red line was archived, but no data was collected along the dashed black lines as these were within the Exclusive Economic Zone (EEZ) of different countries. (b) The ceilometer on the roof deck of the *Shirase* (at the right-bottom corner of the photo).

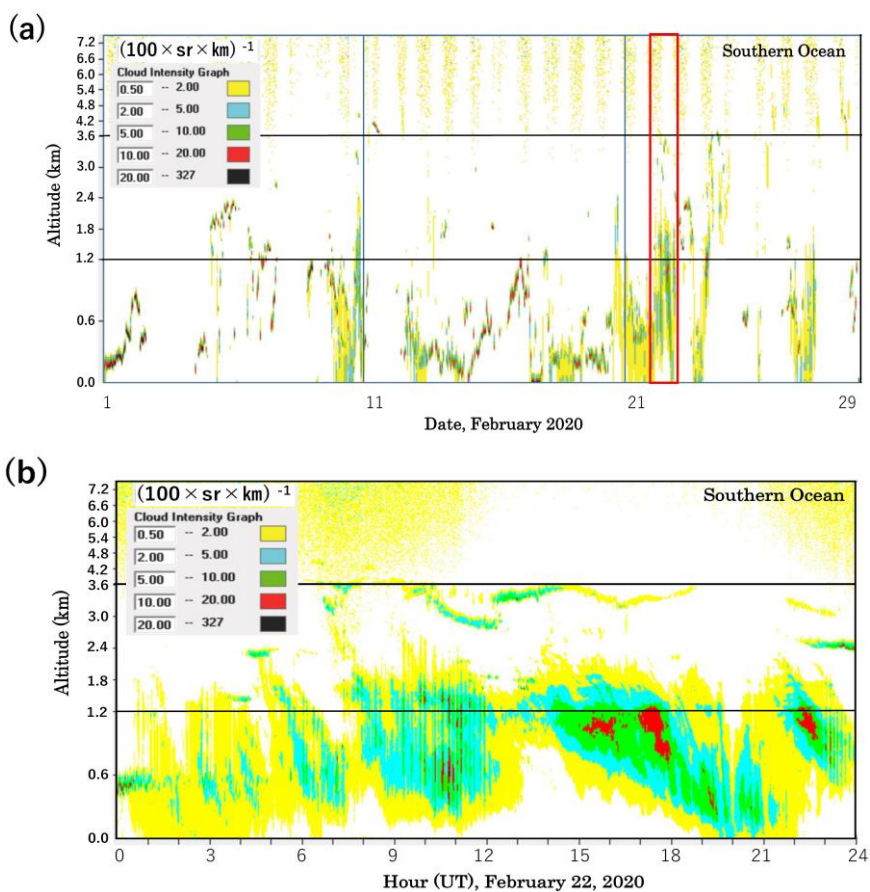


Figure 2. Time-height sections of the backscatters observed by the ceilometer. (a) shows that for February 2020, derived from the annual cruise file of JARE 61 (JARE60_hour.DAT), and (b) for 22 February 2020, derived from the daily file (S00222.DAT). The backscatter coefficients are shown in five different colors according to their magnitude. The red rectangle in (a) indicates 22 February.

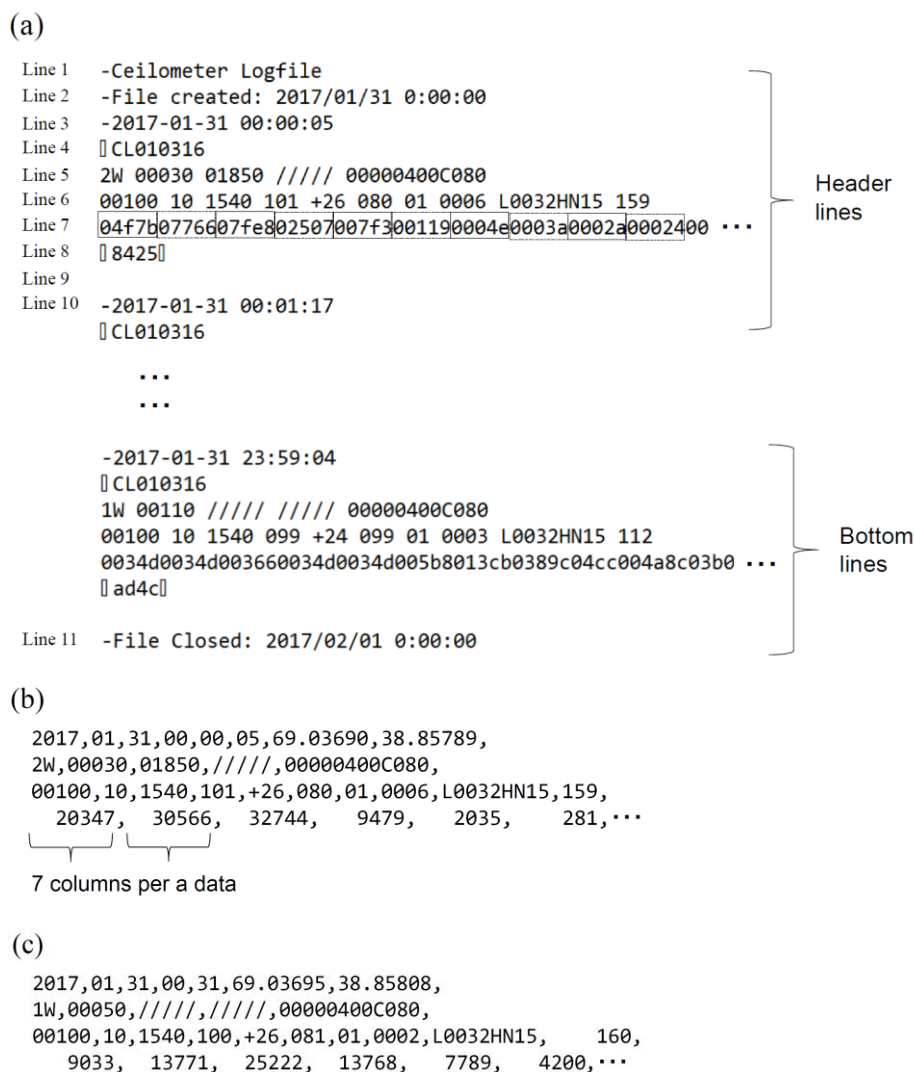


Figure 3. Representative examples of data file formats. (a) The topmost and bottommost lines of the daily file, named “S70131.DAT” (for 31 January 2017), under the directory named “JARE58/0_daily/”. The data are recorded in Vaisala format. (b) The first part of the first line of the “20170131.DAT” (for 31 January 2017) under the directory named “JARE58/10_daily/”. The display is in 4 lines, but they are recorded in 1 line in the actual file. (c) The first part of the data line at 00:00 UT on 31 January 2017 of the annual cruise file, named “JARE58_latlon.DAT”, under the directory named “JARE58/10_all/”. The display is in 4 lines, but they are recorded in 1 line in the actual file.

7. Tables

Table 1. Observation periods for the route over the “North Pacific” after departing from Japan (leftmost column), followed by the route over the Southern Ocean from “Fremantle to Syowa Station”, “Syowa Station”, the route over the Southern Ocean from “Syowa Station to Sydney”, and the route over the “North Pacific” back towards Japan (rightmost column). The Syowa Station area extends from latitude 68°55' S on the outbound route to latitude 68°55' S on the inbound route. Blanks in the data reflect periods when the *Shirase* was within the EEZ of another country. On JARE-57, since the *Shirase* went to Cape Town (*1) after departing from Syowa Station and then went to Sydney (*3) through the Antarctic area (*2), there were the EEZs of South Africa on the cruise route. The letters Y, M, and D indicate the year, month, and date, respectively, and are defined in UTC (Coordinated Universal Time).

JARE	North Pacific				Fremantle to Syowa Station				Syowa Station				Syowa Station to Sydney				North Pacific				
	Y	M	D	Time (UTC)	Y	M	D	Time (UTC)	Y	M	D	Time (UTC)	Y	M	D	Time (UTC)	Y	M	D	Time (UTC)	
52	2010	11	11	05:18	2010	12	1	05:46	2010	12	21	14:16	2011	2	17	06:30					
	-	2010	11	14	23:40	-	2010	12	21	14:16	-	2011	2	17	06:30	-	2011	3	14	10:16	
53	2011	11	11	00:00	2011	12	1	22:10	2012	1	15	04:54	2012	2	22	09:22	2012	3	31	10:16	
	-	2011	11	14	23:24	-	2012	1	15	04:54	-	2012	2	22	09:22	-	2012	3	14	17:22	
54	2012	11	11	00:31	2012	12	1	06:52	2012	12	24	22:45	2013	2	13	14:39					
	-	2012	11	15	19:54	-	2012	12	22	21:59	-	2013	2	13	14:39	-	2013	3	15	01:42	
55					2013	11	28	05:19	2013	12	12	23:07	2014	2	9	07:13	2014	4	2	05:37	
					-	2013	12	12	23:07	-	2014	2	9	07:13	-	2014	3	11	17:22	-	
56	2014	11	1	00:00	2014	12	1	07:39	2014	12	28	10:00									
	-	2014	11	14	20:09	-	2014	12	20	09:59	-	2015	2	9	04:50						
57	2015	11	6	05:00	2015	12	7	10:41	2015	12	21	14:19	*1	2016	2	15	05:12				
	-	2015	11	21	03:57	-	2015	12	21	14:19	-	2016	2	15	05:12	-	2016	2	25	02:37	
																*2	2016	2	27	08:14	
																-	2016	2	29	19:24	
																*3	2016	3	1	12:22	
																-	2016	3	21	03:45	
58	2016	11	1	03:42	2016	12	3	07:24	2016	12	21	06:51	2017	2	15	08:58					
	-	2016	11	16	03:17	-	2016	12	21	06:51	-	2017	2	15	08:58	-	2017	3	17	05:42	
59					2017	12	3	04:25	2017	12	19	10:15	2018	2	15	08:28	2018	4	5	08:50	
					-	2017	12	19	10:15	-	2018	2	15	08:28	-	2018	3	17	05:25	-	
60	2018	11	1	01:43	2018	12	1	06:06	2018	12	20	23:54	2019	2	3	16:35					
	-	2018	11	14	11:11	-	2018	12	20	23:54	-	2019	2	3	16:35	-	2019	3	15	04:28	
61	2019	11	1	00:00	2019	12	3	03:56	2019	12	29	05:36	2020	1	31	08:12	2020	3	31	20:03	
	-	2019	11	16	11:06	-	2019	12	29	05:36	-	2020	1	31	08:12	-	2020	3	16	01:31	
																-	2020	4	14	01:27	

* Y : year, M : month, D : day

*1 Cruise from Syowa Station to Cape Town, South Africa

*2 Cruise from Cape Town to Marion Island, South Africa

*3 Cruise from Marion Island to Sydney, Australia

Table 2. Main specifications of ceilometer measurements

Terms	Values
Laser wavelength	910 nm
Frequency of repetition of the laser emission (Inverse of temporal interval of the laser emission)	6.5 kHz
Temporal interval of measurement	6 s
Temporal interval of recorded data (for this archive)	30 s - 120 s, depending on conditions
Maximum height	15400 m
Spatial interval of the data	10 m
Profile data record format	20 bits (five hexadecimal ASCII)
Cloud base height	Three levels in decimal ASCII

Author contributions

Naohiko Hirasawa processed all the data and acted as the lead in writing the manuscript. Masataka Shiobara designed and organized most of the ceilometer project. Toshiyuki Murayama optimized observations in the early stages of observations. Hiroshi Kobayashi assumed the responsibilities of maintaining stable observation, organizing the group of researchers who participated in this project, and managing observations.

Acknowledgements

We would like to thank Makoto Kuji, Sakiko Ishino, Katsuki Saga, Kouki Saito, Fumihisa Kobayashi, Kazunobu Eryu, Kyohei Yamada, Tetsuro Ojio, Noriaki Tanaka, Masanori Takeda, Junji Matsushita, Shiina Umemoto, and Seiji Koga for operating the instrument on each cruise. Special thanks Tomomi Takamura for organizing the EEZ information and creating a map of the cruising area, and also to Keisuke Saito for helping us create [Table 1](#). We want to thank the editor in charge of this paper and the two anonymous reviewers for their comments, which have improved the quality of this paper. The present study was conducted as one of the scientific projects under the Japanese Antarctic Research Expedition (JARE). The titles of the projects were “Aerosol-mediated material cycle processes in the Antarctic coastal region and the Southern Ocean” (Project No.: AP-11) on JARE-52 (December 2010–March 2011) to JARE-57 (December 2015–March 2016), “Changing of East Antarctic aerosols in the global biogeochemical environment” (Project Nos.: AP0910 and AP0932) and “Mechanism of variation in the surface condition of the ice sheet and heat and moisture budget in east Antarctica” (Project No.: AP0911) on JARE-58 (December 2016–March 2017) to JARE-61 (December 2019–March 2020). Finally, we would like to thank Masahiko Hayashi for supporting this observation as the principal investigator of AP-11, AP0910, and AP0932.

References

1. IPCC, 2021. Climate Change 2021: The Physical Science Basis. Contribution of Working Group I to the Sixth Assessment Report of the Intergovernmental Panel on Climate Change [Masson-Delmotte, V., Zhai, P., Pirani, A., Connors, S. L., Péan, C., Berger, S., Caud, N., Chen, Y., Goldfarb, L., Gomis, M. I., Huang, M., Leitzell, K., Lonnoy, E., Matthews, J. B. R., Maycock, T. K., Waterfield, T., Yelekçi, O., Yu, R., and Zhou, B. (Eds.)]. Cambridge University Press, 2021, 2391 p.
<https://www.ipcc.ch/report/sixth-assessment-report-working-group-i/>.
2. Szopa, S., Naik, V., Adhikary, B., Artaxo, P., Berntsen, T., Collins, W. D., Fuzzi, S., Gallardo, L., Kiendler-Scharr, A., Klimont, Z., Liao, H., Unger, N., and Zanis, P. “Short-Lived Climate Forcers”. Climate Change 2021: The Physical Science Basis. Contribution of Working Group I to the Sixth Assessment Report of the Intergovernmental Panel on Climate Change [Masson-Delmotte, V. *et al.* (Eds.)]. Cambridge University Press, 2021, p. 817–921.
<https://www.ipcc.ch/report/ar6/wg1/chapter/chapter-6/>.
3. Durán-Alarcón, C., Boudevillain, B., Genthon, C., Grazioli, J., Souverijns, N., Van Lipzig, N. P. M., *et al.* The vertical structure of precipitation at two stations in East Antarctica derived from micro rain radars. *The Cryosphere*. 2019, 13(1), p. 247–264. <https://doi.org/10.5194/tc-13-247-2019>.
4. Grazioli, J., Madeleine, J.-B., Gallée, H., Forbes, R. M., Genthon, C., Krinner, G., and Berne, A. Katabatic winds diminish precipitation contribution to the Antarctic ice mass balance. *Proceedings of the National Academy of Sciences*. 2017, 114(41), p. 10858–10863.
<https://doi.org/10.1073/pnas.1707633114>.
5. Hirasawa, N., Konishi, H., Fujiyoshi, Y., Shibata, K., and Iwamoto, K. Snowfall detection by a newly deployed X-band Doppler radar at Syowa Station, Antarctica. *Okhotsk Sea and Polar Oceans Research*. 2022, 6, p. 36–41. <https://doi.org/10.57287/ospor.6.36>.
6. Gorodetskaya, I. V., Kneifel, S., Maahn, M., Van Tricht, K., Thiery, W., Schween, J. H., *et al.* Cloud and precipitation properties from ground-based remote-sensing instruments in East Antarctica. *The Cryosphere*. 2015, 9(1), p. 285–304. <https://doi.org/10.5194/tc-9-285-2015>.
7. Lemonnier, F., Madeleine, J.-B., Claud, C., Genthon, C., Durán-Alarcón, C., Palerme, C., *et al.* Evaluation of CloudSat snowfall rate profiles by a comparison with in situ micro-rain radar observations in East Antarctica. *The Cryosphere*. 2019, 13(3), p. 943–954.
<https://doi.org/10.5194/tc-13-943-2019>.
8. Souverijns, N., Gossart, A., Lhermitte, S., Gorodetskaya, I. V., Grazioli, J., Berne, A., *et al.* Evaluation of the CloudSat surface snowfall product over Antarctica using ground-based precipitation radars. *The Cryosphere*. 2018, 12(12), p. 3775–3789.
<https://doi.org/10.5194/tc-12-3775-2018>.
9. Kuji, M., Fujimoto, R., Miyagawa, M., Funada, R., Hori, M., Kobayashi, H., Koga, S., Matsushita, J., and Shiobara, M. Cloud Fractions Estimated from Shipboard Whole-Sky Camera and Ceilometer Observations. *Trans. JSASS Aerospace Tech. Japan*. 2016, 14, p. 7–13.
https://doi.org/10.2322/tastj.14.Pn_7.

10. Kuji, M., Murasaki, A., Hori, M., and Shiobara M. Cloud Fractions Estimated from Shipboard Whole-Sky Camera and Ceilometer Observations between East Asia and Antarctica. *J. Meteor. Soc. Japan*. 2018, 96, p. 201–214. <https://doi.org/10.2151/jmsj.2018-025>.
11. Vaisala. User's guide, Vaisala Ceilometer CL51. 2010, 118 p.

Data Citations

Hirasawa, N., Shiobara, M., Murayama, T., and Kobayashi, H. (2022): Ship-borne ceilometer measurements over the northwestern Pacific and the Indian sector of the Southern Ocean, and at Syowa Station, Antarctica, in the summers of 2010/11 to 2019/20. *Pol. Data Jour.*, 6, 66–79. <https://doi.org/10.17592/002.2022100393>.